Available online at www.sciencedirect.com

Spectrochimica Acta Part A 70 (2008) 973–982

SPECTROCHIMICA ACTA PART A

www.elsevier.com/locate/saa

# Synthesis, spectroscopic and electrochemical studies on bis-[1,3-substituted (Cl, Br) phenyl-5-phenyl formazanato]nickel(II) complexes

Habibe Tezcan *, Elif Uzluk [1], M. Levent Aksu

*Department of Chemistry, Faculty of Gazi Education, Gazi University, Teknikokullar, 06500 Ankara, Turkey*

Received 23 July 2007; received in revised form 11 September 2007; accepted 4 October 2007

## Abstract

In this study, new 1:2 Ni complexes of 1,3-substituted phenyl-5-phenylformazans were synthesized with –Cl, –Br substituents in the *o*-, *m*-, *p*-positions of the 1-phenyl ring and $-NO_2$ group in the *m*-position of the 3-phenyl ring. Their structures were elucidated and spectral behaviors were investigated with the use of elemental analysis, GC–Mass, $^1H$ NMR, $^{13}C$ NMR, FTIR, UV–vis spectra. Furthermore electrochemical properties such as number of electrons transferred ($n$), diffusion coefficients ($D$) and possible reaction mechanism of the compounds were determined with the use of cyclic voltammetry, ultramicrodisc electrode and chronoamperometry. The relation between their absorption properties and electrochemical properties was examined. A linear correlation was obtained between Hammett substituent coefficients with $\lambda_{max}$ values.

*Keywords:* Formazan dyes; Nickel(II) complexes; Spectroscopy; Substituent effect; Cyclic voltammetry; Ultramicrodiscelectrode; Chronoamperometry

## 1. Introduction

Formazans and their metal complexes are colored compounds due to $\pi$–$\pi^*$ transitions of $\pi$-electrons in formazan skeleton –N=N–C=N–NH– which caused intensive interest among the scientist. There have been numerous formazans synthesized up to now and their structural features, tautomeric and photochromic isomers were investigated [1,2]. Their derivatives with electron donating and withdrawing group attached to 1,3,5-phenyl ring were synthesized and the effects of substituents on the absorption $\lambda_{max}$ values were examined [3,4].

The redox behaviors of formazans were evaluated in detail. Formazans form tetrazolium salt when they are oxidized [5]. Tetrazolium salts are reduced back to formazans by the enzymes in the cell and stain the tissue. Tetrazolium–formazan system is classified as a marker of vitality [6]. This feature enabled the determination of activity on tumor cell [7], which caused an increasing interest in the chemistry, and especially electrochemistry of formazans.

The most comprehensive study related to the redox behavior of formazans was carried out by Umemoto [8]. Here it was claimed that ditetrazolium salts are reduced to both mono and diformazans by 1 electron transfers. The first 1 electron transfer results in the formation of a tetrazolium radical. He claimed that the reaction key leading to the simultaneous generation for mono and diformazans is the disproportionation reaction. It was also claimed that in polarographic study of formazans there were two irreversible diffusion controlled processes, each one with 1 electron transfers [9].

It was reported that formazans are oxidized in a single 2 electron transfer followed by a deprotonation reaction forming corresponding tetrazolium cation [10]. In a study of the reduction of tetrazolium salts into formazans with superoxide ions, claimed to be the cause of aging and various diseases in human body, there was 1 electron transfer at −0.20 V (Ag/AgCl) and one $1e^-/1H^+$ transfer at −0.40 V (Ag/AgCl) [11].

In a previous study the electrochemical behavior of nitro formazan derivatives was investigated and the number of the electrons transferred and diffusion coefficients were determined in a similar manner to the present study. An EC mechanism was proposed involving 1 electron transfer radical formation followed by a tetrazolium anion and cation formation with a disproportional reaction ($TT + e^- + H^+ \Leftrightarrow TT^\bullet$, $TT^\bullet \Leftrightarrow T^+ + T$) [12].

Metal complexes of formazans are colored compounds. That is why they have been subjected to thorough investigation. It

---

* Corresponding author. Tel.: +90 312 2028260; fax: +90 312 2227037.
*E-mail addresses:* habibe@gazi.edu.tr (H. Tezcan), euzluk@yahoo.com (E. Uzluk).

[1] Tel.: +90 312 2028260.

1386-1425/$ – see front matter © 2007 Elsevier B.V. All rights reserved.
doi:10.1016/j.saa.2007.10.010

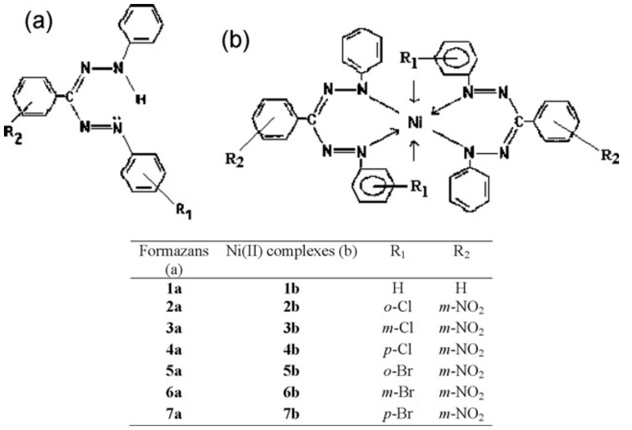

| Formazans (a) | Ni(II) complexes (b) | $R_1$ | $R_2$ |
|---|---|---|---|
| **1a** | **1b** | H | H |
| **2a** | **2b** | *o*-Cl | *m*-$NO_2$ |
| **3a** | **3b** | *m*-Cl | *m*-$NO_2$ |
| **4a** | **4b** | *p*-Cl | *m*-$NO_2$ |
| **5a** | **5b** | *o*-Br | *m*-$NO_2$ |
| **6a** | **6b** | *m*-Br | *m*-$NO_2$ |
| **7a** | **7b** | *p*-Br | *m*-$NO_2$ |

Scheme 1. The structure of the formazans (**a**) and their Ni(II) complexes (**b**) synthesized.

was determined that the formation of Fe complexes was dependent upon the pH value and it was observed that there were two different isomers formed at pH 2 and pH 7–8 [13]. Synthesis, structural determination, stability and formation constants and spectroscopic characterization of metal complexes of formazans were investigated [14–19].

In this study, total seven different novel formazans and their Ni(II) complexes with various substituents on 1- and 3-phenyl rings have been synthesized (Scheme 1). Their structures were elucidated and their spectral behaviors were investigated with the use of elemental analysis, GC–Mass, $^1$H NMR, $^{13}$C NMR, FTIR, UV–vis spectra. The effect of substituents on $\lambda_{max}$ values was determined.

The biological activity of formazan makes the knowledge of its oxidation potentials and possible mechanisms very important. This study is related to the determination of peak potentials, diffusion coefficients ($D$) and a number of electrons transferred ($n$) with the use of cyclic voltammetry, ultramicrodisc electrodes and chronoamperometry. A mechanistic scheme for the oxidation of formazan to tetrazolium salt was proposed based upon these data (Scheme 3).

## 2. Experimental

### 2.1. Chemicals

All chemicals were obtained from Merck and Fluka except sodium hydroxide and [$Ni(CH_3COO)_2 \cdot 4H_2O$] that were purchased from Sigma–Aldrich. All chemicals and solvents used in the syntheses were of reagent grade and were used without further purification. Deionized water (Millipore, Milli-Q) was used for synthesis; the organic solvents, $CH_3OH$, $CH_3OCH_3$, DMSO and dioxane were used for electrochemical and spectroscopic measurements.

### 2.2. Preparation of formazans (*1a*–*7a*)

#### 2.2.1. Synthesis of 1,3,5-triphenylformazan (*1a*)

1,3,5-Triphenylformazan was synthesized by the reaction of benzaldehyde (1.06 g, 0.01 mol), phenylhydrazine (1.08 g, 0.01 mol), aniline (0.93 g, 0.01 mol) concentrated HCl (5 ml) and sodium nitrite (0.75 g) in methanol at 0–5 °C according to literature [2–4]. There was a cherry red colored (**1a**) compound formed. Elemental analysis for $C_{19}H_{16}N_4$ (**1a**): Calc. (%): C, 76.00; H, 5.33; N, 18.66. Found (%): C, 75.97; H, 5.29; N, 18.69. Mass: *m/z* (eV), Calc. *M*: 300.0, Found: *M*: 301.1 ($M^+$). Other peaks: 273.10, 223.00, 195.10, 105.05.

#### 2.2.2. Synthesis of 1-(o-, m-, p-chlorophenyl)-3-(m-nitrophenyl)-5-phenylformazans (*2a*–*4a*)

*m*-Nitrobenzaldehyde (1.51 g, 0.01 mol) was dissolved in methanol (25 ml) and reacted with phenylhydrazine (1.08 g, 00.01 mol) to give *m*-nitrobenzaldehyde phenylhydrazone. The *m*-nitrobenzaldehyde phenylhydrazone (2.41 g, 0.01 mol) was dissolved in methanol (45 ml). In another flask *o*-, *m*-, *p*-chlorobenzenediazonium chloride solutions were prepared using *o*-, *m*-, *p*-nitroaniline (1.27 g, 0.01 mol). This solution was added to the *m*-nitrobenzaldehyde phenylhydrazone solution. The solution was stirred for 2 h at the same temperature and kept in a cupboard for 3 days. Each compound was recrystallised from methanol. There were red-brown colored (**2a**), red-brown colored (**3a**) and dark violet-red colored (**4a**) compounds formed. Elemental analysis for $C_{19}H_{14}N_5O_2Cl$ (**2a**–**4a**): Calc. (%): C, 60.08; H, 3.69; N, 18.44. Found: (%) C, 60.13; H, 3.73; N, 18.50. Mass: *m/z* (eV), Calc. *M*: 379.5, Found: *M*: 380.1 ($M^+$). Other peaks: 274.0, 139.0, 126.0.

#### 2.2.3. Synthesis of 1-(o-, m-, p-bromophenyl)-3-(m-nitrophenyl)-5-phenylformazans (*5a*–*7a*)

*m*-Nitrobenzaldehyde (1.51 g, 0.01 mol) was dissolved in methanol (25 ml) and reacted with phenylhydrazine (1.08 g, 00.01 mol) to give *m*-nitrobenzaldehyde phenylhydrazone. The *m*-nitrobenzaldehyde phenylhydrazone (2.41 g, 0.01 mol) was dissolved in methanol (45 ml). In another flask *o*-, *m*-, *p*-bromobenzenediazonium chloride solutions were prepared using *o*-, *m*-, *p*-nitroaniline (1.27 g, 0.01 mol). This solution was added to the *m*-nitrobenzaldehyde phenylhydrazone solution. The procedure was as alike as early in Section 2.2.2. There were dark orange-red (**5a**), dark red colored (**6a**) and orange-red colored **7a** formed. Elemental analysis for $C_{19}H_{14}N_5O_2Br$ (**5a**–**7a**), Calc. (%): C, 53.77; H, 3.30; N, 16.51. Found: (%) C, 53.70; H, 3.27; N, 16.55. Mass: *m/z* (eV), Calc. *M*: 424.0, Found *M*: 425.0 ($M^+$). Other peaks: 318.3, 240.0, 170.1.

### 2.3. Synthesis of the nickel(II) complexes

#### 2.3.1. Synthesis of bis (1,3,5-triphenyl formazanato)nickel(II) complexes (*1b*)

1,3,5-Triphenylformazan (**1a**) (1.500 g, 0.005 mol) obtained as outlined in Section 2.2 was dissolved in dioxane (20 ml). In another flask [$Ni(CH_3COO)_2 \cdot 4H_2O$] salt (0.0025 mol, 0.625 g) was dissolved in ethanol (25 ml) under reflux with constant stirring at 25 °C and formazan solution was added to it. There was no color change or precipitation observed during this process. The mixture was stirred for 8 h with a magnetic stirrer at 30–35 °C under reflux. The precipitation started after an hour and the color

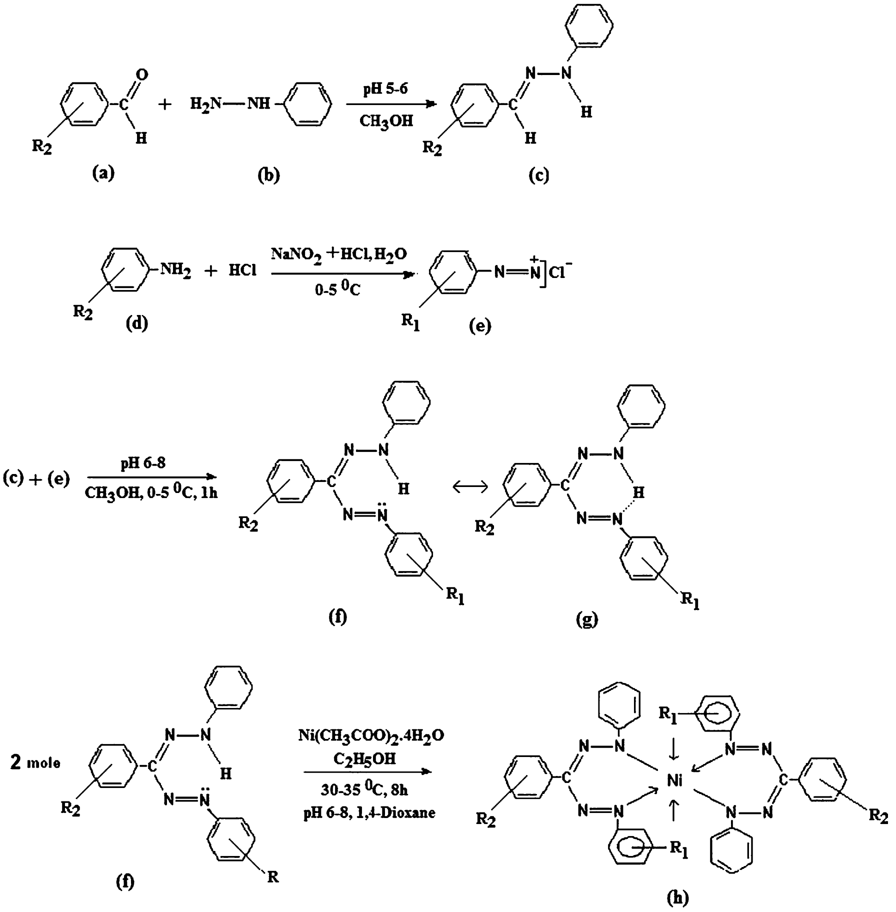

Scheme 2. Synthesis of formazans and their Ni(II) complexes.

turned into orange from red after 2 h and brown after 3 h. The color remained brown. The mixture was kept in the cupboard for 4 days. The light-brown precipitate was filtered off and washed with 10 ml 0.5 M NaOH, water and methanol. The compound was dried in stove at 40 °C for 24 h and recrystallized from methanol.

### *2.3.2. Synthesis of bis-[1-(o-, m-, p-chlorophenyl)-3-(m-nitrophenyl)-5-phenyl formazanato]nickel(II) complexes (2b–4b)*

Formazans (**2a**–**4a**) (0.760 g, 0.002 mol) obtained as described in Section 2.2 were dissolved in dioxane (25 ml). In another flask [Ni($CH_3COO)_2\cdot 4H_2O$] (0.001 mol, 0.250 g) salt was dissolved in ethanol (15 ml) and formazan solutions were added to it. The mixtures were stirred at 30–35 °C under reflux for 8 h. The resulting precipitates were kept in the cupboard for 3 days. The brown colored (**2b**), light green colored (**3b**) and brown colored (**4b**) products were filtered off, washed with water and methanol, recrystallized from methanol and dried in stove at 40 °C for 24 h. Elemental analysis for $C_{40}H_{34}N_{10}O_6Cl_2Ni$, *M*: 880.37. Calc. (%): C, 54.57; H, 3.89; N, 15.91. Found: (%) C, 54.53; H, 3.92; N, 17.85. Mass: *m*/*z* (eV), Calc. *M*: 880.37. Found *M*: 880.40 ($M^+$). Other peaks: 437.20, 378.05, 240.05.

### *2.3.3. Synthesis of bis [1-(o-, m-, p-bromophenyl)-3-(m-nitrophenyl)-5-phenyl formazanato]nickel(II) complexes (5b–7b)*

Formazans (**5a**–**7a**) (0.848 g, 0.002 mol) prepared in Section 2.2 was dissolved in ethanol (10 ml) and dioxane (25 ml). In another flask [Ni($CH_3COO)_2\cdot 4H_2O$] (0.001 mol, 0.250 g) salt was dissolved in ethanol (15 ml) and formazan solution was added to it. Following a similar procedure as in Section 2.3.2 and the brown colored (**5b**), light green-brown (**6b**) and brown colored (**7b**) were filtered off and recrystallized from dioxane. Elemental analysis for $C_{40}H_{34}N_{10}O_6Br_2Ni$, *M*: 969.27. Calc. (%): C, 49.57; H, 3.54; N, 14.44. Found: (%) C, 49.52; H, 3.57; N, 14.48. Mass: *m*/*z* (eV), Calc. *M*: 969.27. Found *M*: 969.40 ($M^+$). Other peaks: 481.15, 423.90, 240.90. The reaction scheme is given in Scheme 2 and the experimental parameters are tabulated in Table 1.

### *2.4. Physical measurements*

The UV–vis spectra of the formazans synthesized in this study were obtained with UNICAM UV2-100 UV–vis spectrophotometer using 1 cm quartz cells in $10^{-5}$ mol l$^{-1}$ DMSO using a 325 nm lamp in the range of 250–600 nm. The IR spectra were obtained on a MATT-SON 100-FT-IR spectrophotometer

Table 1
Experimental and $^{1}$H NMR data of the Ni(II) complexes formazans (**1b**–**7b**) investigated

| Compound | Color | m.p. (°C) | Yield (%) | $^{1}$H NMR data[a] Aromatic H/$\delta$ (ppm) |
|---|---|---|---|---|
| **1b** | Light brown | 300 | 85 | 8.02–7.28(30H) |
| **2b** | Pink-brown | 240 | 79 | 8.82–7.30(26H) |
| **3b** | Light green | 305 | 65 | 8.45–7.12(26H) |
| **4b** | Brown | 310 | 63 | 8.78–7.22(26H) |
| **5b** | Pink-brown | 260 | 82 | 8.84–7.24(26H) |
| **6b** | Light green | 281.5 | 63 | 8.50–7.02(26H) |
| **7b** | Brown | 298 | 60 | 8.62–7.30(26H) |

[a] The $^{1}$H NMR spectra were recorded with 400 MHz (in $CDCl_3$).

between 4000 and 400 cm$^{-1}$ using KBr pellets. $^{1}$H NMR spectra were performed on a Bruker AVANCE DPX-400 MHz and $^{13}$C NMR 100 MHz spectrophotometer using $CDCl_3$ and $d_6$-DMSO, $10^{-4}$ mol l$^{-1}$. The elemental analyses were carried out by the use of LECO-CHNS-932 elemental analyzer. Mass spectra were recorded using an AGILENT 1100 MSD mass spectrometer. Electrochemical studies were carried out on a computerized CHI Instrument 660 B system in a conventional three-electrode cell. A platinum electrode (PE) (CHI102) and a 10 μm-platinum ultramicro electrode (UME) (CHI107) were used as a working electrode. The electrodes were cleaned by electrochemical potential cycling and washing with excess dimethyl sulfoxide. A platinum wire was used as the auxiliary electrode. The reference electrode was a silver wire in contact with 0.1 M $AgNO_3$ in dimethyl sulfoxide. All solutions were deaired for 10 min with pure argon. All the measurements were taken at room temperature, 25 °C. The supporting electrolyte, tetrabutylammonium tetrafluoroborate (TBATFB) was purchased from Fluka (21796-4) and was used without purification. DMSO was used, as solvent, ionic strength was maintained at 0.1 M, with TBATFB as supporting electrolyte. The concentration of all species was $1 \times 10^{-4}$ M.

## 3. Results and discussion

The analytical data of the Ni complexes of formazan indicate 1:2 metal to ligand stoichiometry. All the isolated complexes are stable in air, in anhydrous EtOH and MeOH, but soluble in DMSO and DMF. Attempts to propose the structure of the isolated complexes come from full investigation using the following studies.

### 3.1. $^{1}$H NMR spectra

When one examines $^{1}$H NMR data listed in Table 1 shows that the aromatic-H peak for Ni-TPF (**1b**) are observed at $\delta = 8.02$–7.28 ppm. In Ni(II) complexes formazans (**2b**–**4b**; **5b**–**7b**) where position of the 3-phenyl ring is substituted with *m*-$NO_2$ while –Cl, –Br is each substituted to *o*-, *m*-, *p*-positions of 1-phenyl ring, the aromatic-H signals 8.82, 8.45, 8.78 ppm; 8.84, 8.50, 8.62 ppm, respectively are shifted towards lower fields according to Ni-TPF (**1b**). This is in good accordance with the electron withdrawing properties of these substitutes. When aromatic-H peaks Ni(II) complexes are compared with the corresponding formazans they were observed to shift towards lower fields. This is in accordance with the fact that the electrons in the structure are withdrawn with the insertion of $Ni^{2+}$ into formazans structure [16,22,23]. N–H peak observed in formazans were absent in Ni(II) complexes. This the further proof that metal is replaced in place of proton of N–H group. These data are supported with IR results.

Table 2
$^{13}$C NMR data of the Ni(II) complexes formazans (**1b**–**7b**) investigated (in $CDCl_3$ and DMSO-$d_6$)

| Compound | $\delta$ (ppm) | |
|---|---|---|
| | Imino-C (C═N) | Other carbons |
| **1b** | 174.81 | 163.97, 161.86, 158.67, 157.90, 155.03, 153.47, 152.20, 150.21, 149.01, 148.61, 142.21, 139.03, 130.42, 127.90, 126.33, 120.59, 118.50 (total 20C) |
| **2b** | 175.31 | 167.81, 163.90, 150.94, 149.69, 147.96, 146.72, 145.62, 144.53, 143.75, 143.12, 141.72, 141.09, 140.62, 139.75, 137.75, 137.00, 134.50, 133.25, 132.75, 131.25, 130.00, 128.75, 127.00, 126.25, 125.10, 124.50, 123.00, 122.50, 122.00, 120.15, 116.00, 113.50, 108.20 (total 34C) |
| **3b** | 175.36 | 172.06, 164.80, 160.00, 153.05, 149.44, 148.89, 148.33, 147.22, 145.56, 144.17, 143.33, 142.50, 141.39, 140.00, 139.17, 137.50, 136.39, 135.28, 134.44, 133.89, 132.50, 131.11, 130.00, 128.06, 127.67, 125.10, 124.17, 123.33, 122.78, 121.67, 121.39, 119.78, 116.28 (total 34C) |
| **4b** | 174.80 | 172.36, 163.85, 149.44, 148.33, 146.67, 145.00, 144.44, 143.33, 142.22, 141.11, 139.89, 137.78, 136.67, 135.47, 134.44, 133.89, 132.78, 131.11, 130.23, 129.79, 128.89, 127.78, 125.56, 122.22, 120.38, 119.44, 117.22, 115.00, 110.00 (total 30C) |
| **5b** | 172.38 | 164.87, 163.32, 150.15, 149.61, 149.00, 148.65, 147.11, 146.15, 145.38, 144.42, 143.07, 141.73, 140.96, 140.19, 139.42, 137.88, 135.70, 135.00, 134.42, 133.27, 131.92, 130.96, 129.42, 128.65, 127.50, 126.54, 125.00, 124.04, 122.50, 121.54, 118.85, 115.58, 107.52 (total 34C) |
| **6b** | 175.02 | 170.38, 164.86, 152.86, 151.07, 148.57, 146.43, 145.71, 144.98, 143.57, 142.14, 141.07, 139.29, 138.57, 136.43, 135.10, 134.28, 133.57, 131.78, 130.71, 130.00, 129.28, 127.78, 127.50, 126.79, 126.07, 125.00, 120.00, 119.28, 117.14, 115.00, 112.88, 111.07, 108.57 (total 34C) |
| **7b** | 174.96 | 167.47, 156.50, 149.38, 149.00, 148.17, 147.50, 146.53, 145.97, 145.00, 144.50, 143.25, 142.80, 141.53, 140.82, 140.10, 139.50, 139.38, 138.50, 136.65, 135.00, 134.81, 129.17, 126.10, 124.64, 122.50, 120.00, 117.22, 113.90, 110.88 (total 30C) |

Table 3
The IR data of the Ni(II) complexes formazans (**1b**–**7b**) (in KBr, $cm^{-1}$)

| Compound | Aromatic C–H | Aromatic C=C | C=N | N=N | N–Ni | CNNC structural vibration |
|---|---|---|---|---|---|---|
| **1b** | 3098–3025 | 1600 | 1500 | 1410 | 3089 | 780–550 |
| **2b** | 3482–3384 | 1589 | 1527 | 1241 | 2938 | 813–652 |
| **3b** | 3482–3428 | 1607 | 1563 | 1276 | 2987 | 830–679 |
| **4b** | 3480–3410 | 1607 | 1536 | 1277 | 2945 | 857–679 |
| **5b** | 3491–3411 | 1598 | 1527 | 1232 | 3010 | 813–652 |
| **6b** | 3490–3464 | 1580 | 1536 | 1214 | 2980 | 800–650 |
| **7b** | 3490–3411 | 1571 | 1527 | 1276 | 2965 | 813–643 |

### 3.2. $^{13}C$ NMR spectra

As seen from Table 2, the δ value for C=N carbon of Ni-TPF complex (**1b**) is 174.81 ppm. The attachment of a second electron withdrawing group (–Cl, –Br) to *o*-, *m*-, *p*-position of the 1-phenyl ring while 3-phenyl ring contains an electron withdrawing group *m*-$NO_2$ does not cause a significant change in δ values. C=N carbon peaks of Ni(II) complexes are in lower fields compared with those of corresponding formazans. While C=N peaks observed between 149.61 and 150.82 ppm in formazans are shifted to 172.38–175.36 ppm in Ni(II) complexes. This result is in accordance with the replacement of an electron withdrawing $Ni^{2+}$ into the system. Other C peaks can also be evaluated in a similar manner [17].

### 3.3. IR spectral studies

As seen in Table 3, the C=N stretching band of Ni-TPF (**1b**) was observed at 1500 $cm^{-1}$. The band related to the *o*-,*m*-, *p*-substituted Cl (**2b**–**4b**) on 1-phenyl ring were observed at 1527, 1563 and 1536 $cm^{-1}$. These peaks appeared at 1527, 1536, 1527 $cm^{-1}$ in the case of *o*-, *m*-, *p*-Br substitution (**5b**–**7b**). The C=N bands observed at 1530–1520 $cm^{-1}$ in formazans were observed to shift to 1563–1527 $cm^{-1}$ in Ni(II) complexes. The N–H band observed at 3120–2850 $cm^{-1}$ in formazans was observed to disappear in their Ni(II) complexes. However new peaks appeared at 3089–2938$cm^{-1}$. These peaks were attributed to metal–ligand bonds. This is the verification of the formation of Ni(II) complexes as a result of replacement of $Ni^{2+}$ in place of H atom in N–H [17]. These results confirm the formula given in Scheme 1. However the N–H band was weakly observed in compound (**3b**). These results are in agreement with literature [15]. N=N band observed at 1410 $cm^{-1}$ Ni-TPF (**1b**). This band was seen to shift to 1241, 1276 and 1277 $cm^{-1}$ in *o*-, *m*-, *p*-Cl substituted Ni(II) complexes (**2b**–**4b**) and 1232, 1214 and 1276 $cm^{-1}$ *o*-, *m*-, *p*-Br substituted Ni(II) complexes (**5b**–**7b**). N=N band was observed to shift towards the lower frequencies in Ni-TPF (**1b**) than their respective formazan (**1a**). This band also shifted to lower frequencies in Cl and Br substituted formazans. Ni(II) complexes compared to Ni-TPF (**1b**). The results are in agreement with literature [17]. Other aromatic C–H, C=C, CNNC skeleton stretching peaks in all complexes were observed in their expected regions [24]. The changes in bands belonging to C=N, N–H and N=N groups taking **6a** and **6b** as an example are shown in Fig. 1.

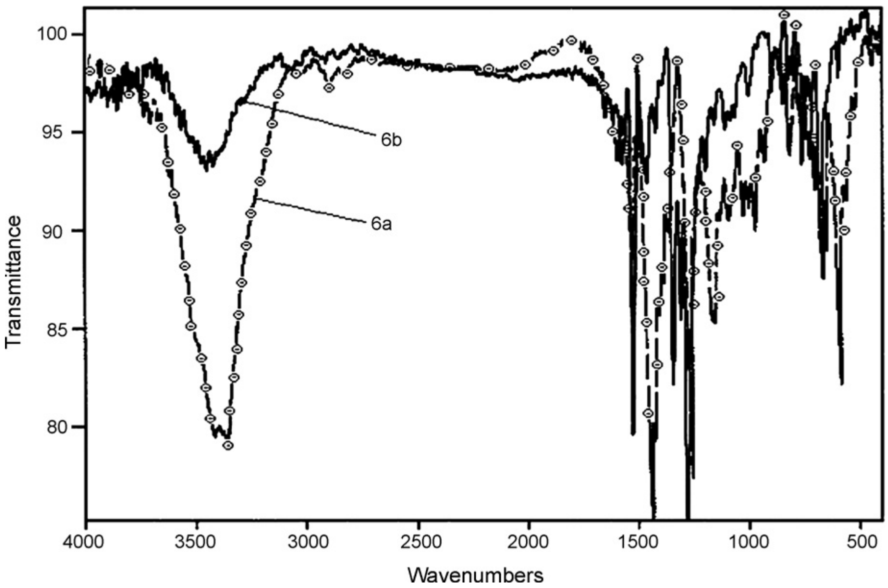

Fig. 1. Comparison the IR bands of compounds (**6a** and **6b**).

Table 4
UV–vis absorption maxima of the Ni(II) complexes formazans (**1b**–**7b**) (DMSO, $\times 10^{-5}$ mol/l)

| Compound | Abbreviation | $\lambda_{max1}$ (nm) (Abs) | $\lambda_{max2}$ (nm) (Abs) | $\lambda_{max3}$ (nm) (Abs) | Chemical shift $\Delta\lambda_{max}$ |
|---|---|---|---|---|---|
| **1b** | Ni-TPF | 611.0 (0.067) | 481.0 (0.684) | 275.0 (0.722) | – |
| **2b** | Ni-*o*-CNF | 621.0 (0.032) | 481.0 (0.740) | 305.0 (1.338) | 10 |
| **3b** | Ni-*m*-CNF | 619.0 (0.063) | 415.6 (0.548) | – | 8 |
| **4b** | Ni-*p*-CNF | 624.0 (0.058) | 426.0 (0.402) | 275.0 (1.423) | 13 |
| **5b** | Ni-*o*-BNF | 622.0 (0.054) | 479.0 (0.617) | 304.0 (1.176) | 11 |
| **6b** | Ni-*m*-BNF | 618.0 (0.064) | 413.4 (0.452) | 298.0 (1.164) | 7 |
| **7b** | Ni-*p*-BNF | 625.1 (0.047) | 415.8 (0.354) | 355.0 (0.648) | 14 |

Column 6: $\Delta\lambda_{max} = \lambda_{max1}$(Ni-TPF) − $\lambda_{max1}$ (substituted Ni(II) complexes formazans).

### 3.4. Substituent effect on the UV–vis absorption $\lambda_{max}$ values

As seen from Table 4 there were three peaks observed in the UV–vis spectra of the Ni(II) complexes of formazans. The absorptions peaks are: $\lambda_{max1}$ the Ni(II) complex unit, $\lambda_{max2}$ formazan unit and $\lambda_{max3}$ hydrazone unit were attributed [8,20,21]. The $\lambda_{max1}$ values observed at 479–486 nm in formazans shifted to 611–625.1 nm in Ni(II) complexes. This is an expected outcome as a result of the replacement of the Ni(II) ion in the structure. These results are in agreement with literature [15,16,18,20]. When $\Delta\lambda_{max}$ values are compared according to the type of the substituents it was observed that the value of shift is almost the same with the presence of Cl and Br. This was an expected outcome since the electron withdrawing inductive and electron donating resonance effects approximately cancel each other. The small difference (1 nm) between them may be the manifestation of the difference in their respective electronegativity values. When $\lambda_{max}$ values are compared according to the positions of the substituents at the 1-phenyl ring of the complexes containing Cl and Br followed the order of *p*- > *o*- > *m*-positions. If we think that electron withdrawing effect results only from the inductive effect which diminishes as move from the center and resonance effect will be dominant *o*-position and *p*-position are expected outcome. These results are depicted in Fig. 2a and b. All these shift values ($\lambda_{max}$) are illustrated in Fig. 3 for comparative purpose.

### 3.5. Mass spectra

The mass spectra of formazans (**1a**–**7a**) and their complexes (**1b**–**7b**) were recorded and their moleculer ion peaks confirm the suggested formula of these formazans and their complexes (Scheme 1). The calculated and found values of the moleculer weigths of the formazans and their nickel complexes are given in Section 2. Elemental analysis and mass spectroscopic data corroborated the structures proposed in Scheme 1.

### 3.6. Cyclic voltammetry

The electrochemistry of formazans substituted with *o*-, *m*-, *p*-Cl and –Br at the 1-phenyl and *m*-$NO_2$ at the 3-phenyl ring were discussed in detail in our previous study. The cyclic voltammograms of their corresponding Ni(II) complexes are given in Figs. 4 and 5.

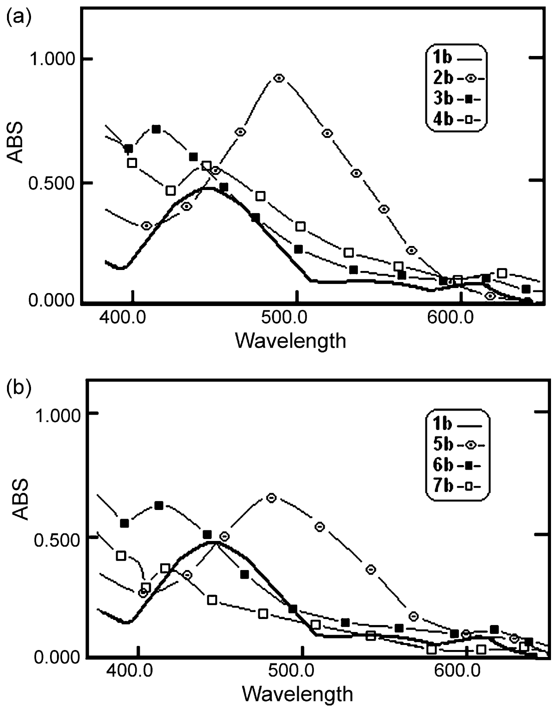

Fig. 2. Absorption spectra of: (a) $1.0 \times 10^{-5}$ M DMSO solutions of compounds (**2b**–**4b**) compared to Ni-TPF (**1b**) and $1.0 \times 10^{-5}$ M DMSO solutions of compounds (**5b**–**7b**) compared to Ni-TPF (**1b**).

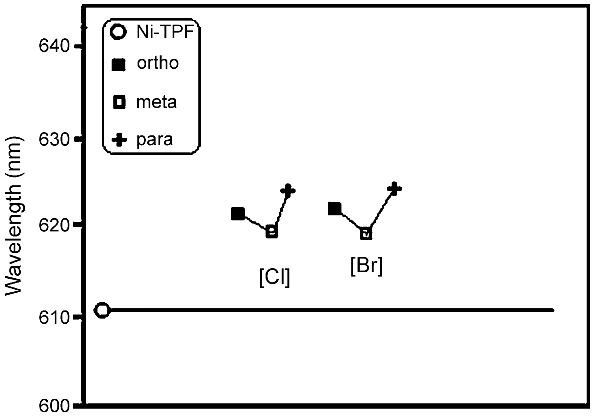

Fig. 3. The comparison of the absorption values of substituted Ni(II) complexes formazans (**2b**–**7b**) against Ni-TPF (**1b**).

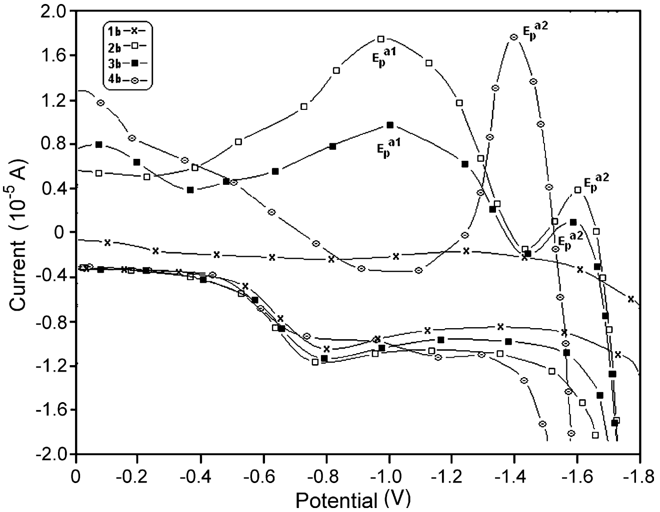

Fig. 4. Cyclic voltammogram of DMSO solutions of $1.0 \times 10^{-4}$ M compounds (**1b**–**4b**) in the presence of 0.1 M TBATFB at Pt electrode. Potential scan rate: 100 mV s$^{-1}$.

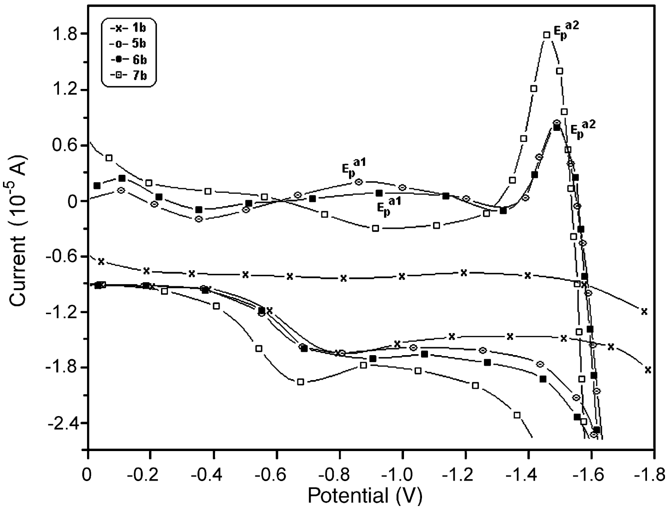

Fig. 5. Cyclic voltammogram of DMSO solutions of $1.0 \times 10^{-4}$ M compounds (**1b**, **5b**–**7b**) in the presence of 0.1 M TBATFB at Pt electrode. Potential scan rate: 100 mV s$^{-1}$.

As seen from Fig. 4 Ni-TPF (**1b**) gave no anodic peak in the forward direction. However shows that the substituted groups have a quite effect upon the electrochemical behavior of the formazan Ni(II) complexes. There are a broad peak at −967 mV and a much sharper peak at −1605 mV for the *o*-Cl substituted formazan complex (**2b**). This suggests that the complex give tetrazolium cation by two successive electron transfers. The same situation exists for *m*-Cl substituted formazan Ni(II) complex (**3b**). However, the intensities of the first and second peaks are much lower compared with to the *o*-Cl substituted Ni(II) complex. This shows that the electron transfer rate is much lower in *m*-Cl substituted Ni(II) complexes. The appearance of the voltammogram for *p*-Cl substituted formazan Ni(II) complex (**4b**) is highly different. The first peak observed around −1000 mV for *o*-, *m*-Cl is absent in *p*-Cl Ni(II) complex. The intensity of the second peak is much higher for the *p*-Cl substituted complex compared with those of *o*-and *m*-Cl substituted complexes. This may be explained by the decreasing inductive effect going from *o*- to *p*-position.

The second peak showed a shift of 200 mV towards anodic direction for *p*-Cl substituted Ni(II) complex compared to *o*-, *m*-Cl substituted complexes and appears at −1396 mV. This shift may be the result of higher electronegativity of Cl (this shift is much lower in Br complexes as will be outlined shortly). This is the indicative of the fact that *p*-Cl complex directly gives a tetrazolium cation by a single step 2 electron transfer. On the other hand *o*- and *m*-substituted complexes give two successive 1 electron transfer giving tetrazolium cation *via* radical ion. The intensity of the first peak changes as *o*- > *m*- > *p*-Cl substituted Ni(II) complexes. This is in accordance with the yield of *p*-Cl substituted complex was the highest followed by *m*-Cl and *o*-Cl substituted Ni(II) complexes. These results also are in accordance with the spectroscopic data. The same arguments made for Cl are valid for Br as well. The only exception is that the shift in the sharp peak observed in the reverse scan is smaller with the *p*-substituted Br compared to *p*-Cl substituted Ni(II) complex which was attributed to lower electronegativity of Br compared to Cl. The results are in good accordance with the spectroscopic data. All the cyclic voltammetric data are tabulated in Table 5.

### 3.7. Ultramicro disc and chronoamperometric results

The number of electrons transferred was found with the use of chronoamperometric, Cottrell equation and ultra micro Pt disc electrode (UME) steady state current [20]. The real surface area of the Pt electrode was found to be 2.58 cm$^2$ with the use ferrocene. If $i_t$ values are plotted against $t^{-1/2}$ the resulting slope

Table 5
Voltamperometric results in DMSO at 25 °C in platinum electrode, ionic strength 0.1 M (TBATFB), sweep speed: 100 mV s$^{-1}$. $E_p^{a1}$: anodic, $E_p^{a2}$: anodic

| Compound | Abbreviation | First peak | | Second peak | |
|---|---|---|---|---|---|
| | | $E_p^{a1}$ (mV) | $I_p^1$ (A) | $E_p^{a2}$ (mV) | $I_p^2$ (A) |
| **1b** | Ni-TPF | – | – | – | – |
| **2b** | Ni-*o*-CNF | −967.0 | $1.637 \times 10^{-5}$ | −1605 | $2.884 \times 10^{-6}$ |
| **3b** | Ni-*m*-CNF | −1008.0 | $1.876 \times 10^{-6}$ | −1585 | $1.400 \times 10^{-7}$ |
| **4b** | Ni-*p*-CNF | – | – | −1396 | $1.680 \times 10^{-5}$ |
| **5b** | Ni-*o*-BNF | −873.0 | $6.823 \times 10^{-6}$ | −1461 | $2.282 \times 10^{-5}$ |
| **6b** | Ni-*m*-BNF | −893.5 | $5.822 \times 10^{-6}$ | −1494 | $1.315 \times 10^{-5}$ |
| **7b** | Ni-*p*-BNF | – | – | −1338 | $1.338 \times 10^{-5}$ |

Table 6
Some of the parameters calculated for Ni(II) complexes formazans

| Compound | Abbreviation | $C^*$ (ml) | $\dot{I}_{ss}$ (A) | Cottrell slope (S) | $n$ | $n$ net | $D$ (cm$^2$/s) |
|---|---|---|---|---|---|---|---|
| **1b** | Ni-TPF | 7.8 | $4.417 \times 10^{-10}$ | $1.249 \times 10^{-5}$ | 0.88 | 1 | $1.667 \times 10^{-6}$ |
| **2b** | Ni-*o*-CNF | 8.0 | $2.782 \times 10^{-10}$ | $1.457 \times 10^{-5}$ | 1.85 | 2 | $4.864 \times 10^{-5}$ |
| **3b** | Ni-*m*-CNF | 9.1 | $2.358 \times 10^{-10}$ | $1.417 \times 10^{-5}$ | 1.82 | 2 | $3.356 \times 10^{-7}$ |
| **4b** | Ni-*p*-CNF | 8.8 | $3.917 \times 10^{-10}$ | $1.822 \times 10^{-5}$ | 1.87 | 2 | $6.166 \times 10^{-5}$ |
| **5b** | Ni-*o*-BNF | 8.3 | $4.543 \times 10^{-10}$ | $2.194 \times 10^{-5}$ | 2.48 | 2 | $5.720 \times 10^{-5}$ |
| **6b** | Ni-*m*-BNF | 8.5 | $7.082 \times 10^{-10}$ | $6.875 \times 10^{-6}$ | 1.52 | 2 | $1.079 \times 10^{-6}$ |
| **7b** | Ni-*p*-BNF | 7.4 | $4.375 \times 10^{-10}$ | $1.053 \times 10^{-5}$ | 0.66 | 1 | $2.303 \times 10^{-6}$ |

will be from which $n$ could easily be calculated. The calculated $n$ values are given in Table 6.

Looking at the UME results (Figs. 6 and 7) there is a 1 electron transfer wave for Ni-TPF (**1b**). Ni-TPF (**1b**) is fragmented. $Ni^{2+}$ and $TF^-$ anion (**X**) occurred in solution (Scheme 3). $TF^-$ anion gives a single 1 electron transfer giving a formazan radical ($TF^\bullet$). These radicals probably give a disproportionation reaction to give a formazan and $TTC^+$ cation or a dimerization reaction resulting a diformazan. Mechanism of the oxidation of compound (**1b**) is shown in Scheme 3A and B. These results are in agreement with literature [8,12].

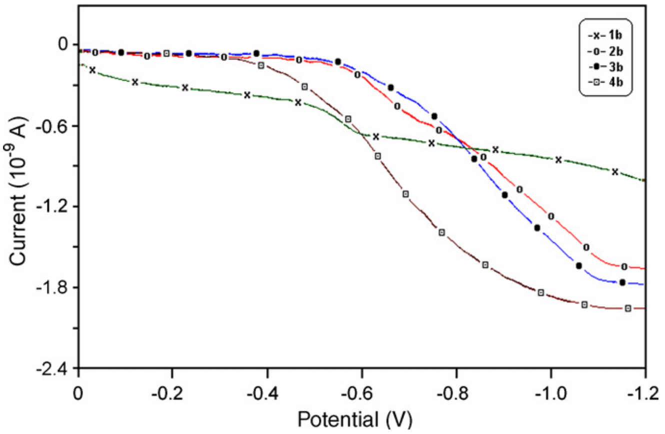

Fig. 6. UME curves of Ni-TPF (**1b**) and compounds (**2b**–**4b**) at 10 μm-platinum ultramicroelectrode. Potential scan rate: 10 mV s$^{-1}$.

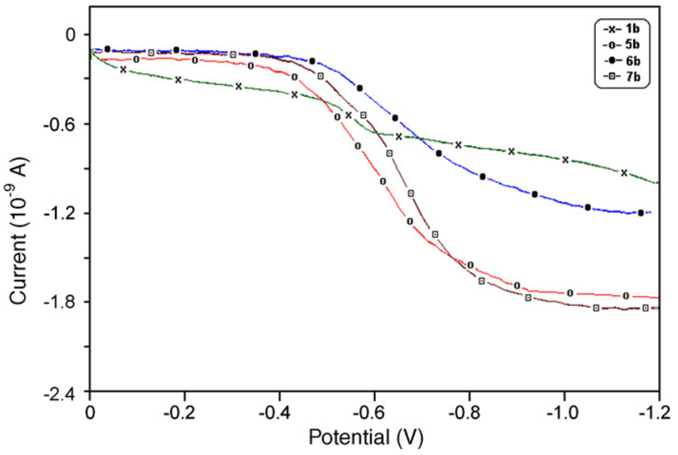

Fig. 7. UME curves of Ni-TPF (**1b**) and compounds (**5b**–**7b**) at 10 μm-platinum ultramicroelectrode. Potential scan rate: 10 mV s$^{-1}$.

Both the complexes of Cl and Br substituted formazans gave clear S-shaped steady state currents with UME (Figs. 6 and 7). The number of electrons transferred was found to be in accordance with the CV data. The diffusion coefficients were also found within expected dimensions. The results of UME and chronoamperometric data are tabulated in Table 6.

The number of electrons transferred is two for all *o*-, *m*-, *p*-Cl substituted Ni(II) complexes based on UME and chronoamperometric. This is in accordance with CV results. The appearance of two distinctive peaks in cyclic voltammograms of *o*-, *m*-Cl substituted Ni(II) complexes suggest that the compounds give two successive 1 electron transferred giving formazan radical and tetrazolium cation. Mechanism of the oxidation of *o*-, *m*-Cl substituted Ni(II) complexes (**2b**, **3b**) are shown in Scheme 3C. These results are in agreement with literature [11]. However the presence of only one peak in the case of *p*-substituted Ni(II) complex (**4b**) is most probably due to the fact of the compound giving a 2 electron transfer resulting directly into the tetrazolium cation. Mechanisms of the oxidation of compounds (**4b**) are shown in Scheme 3D. These results are in agreement with literature [10]. The situation for *o*-, *m*-Br substituted Ni(II) complexes (**5b**, **6b**) are the same with Cl-substituted Ni(II) complexes. Mechanism of the oxidation of *o*-, *m*-Br substituted Ni(II) complexes (**5b**, **6b**) are shown in Scheme 3C. These results are in agreement with literature [11]. However *p*-Br substituted Ni(II) complex (**7b**) appears to make 1 electron transfer. This complex probably gives dimerization or disproportionation reaction following the radical formation step. Mechanism of the oxidation of compound (**7b**) is shown in Scheme 3A, B. These results are in agreement with literature [8,12].

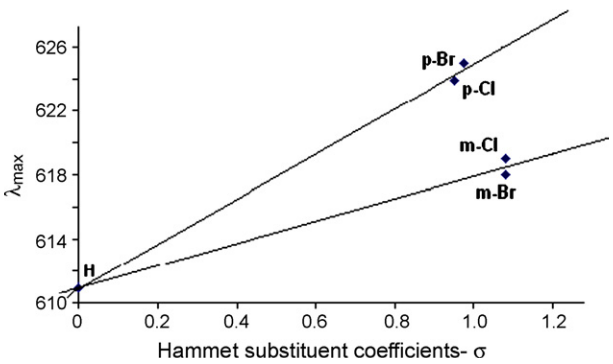

Fig. 8. The $\lambda_{max}$ values against the Hammett substituent coefficients-$\sigma$.

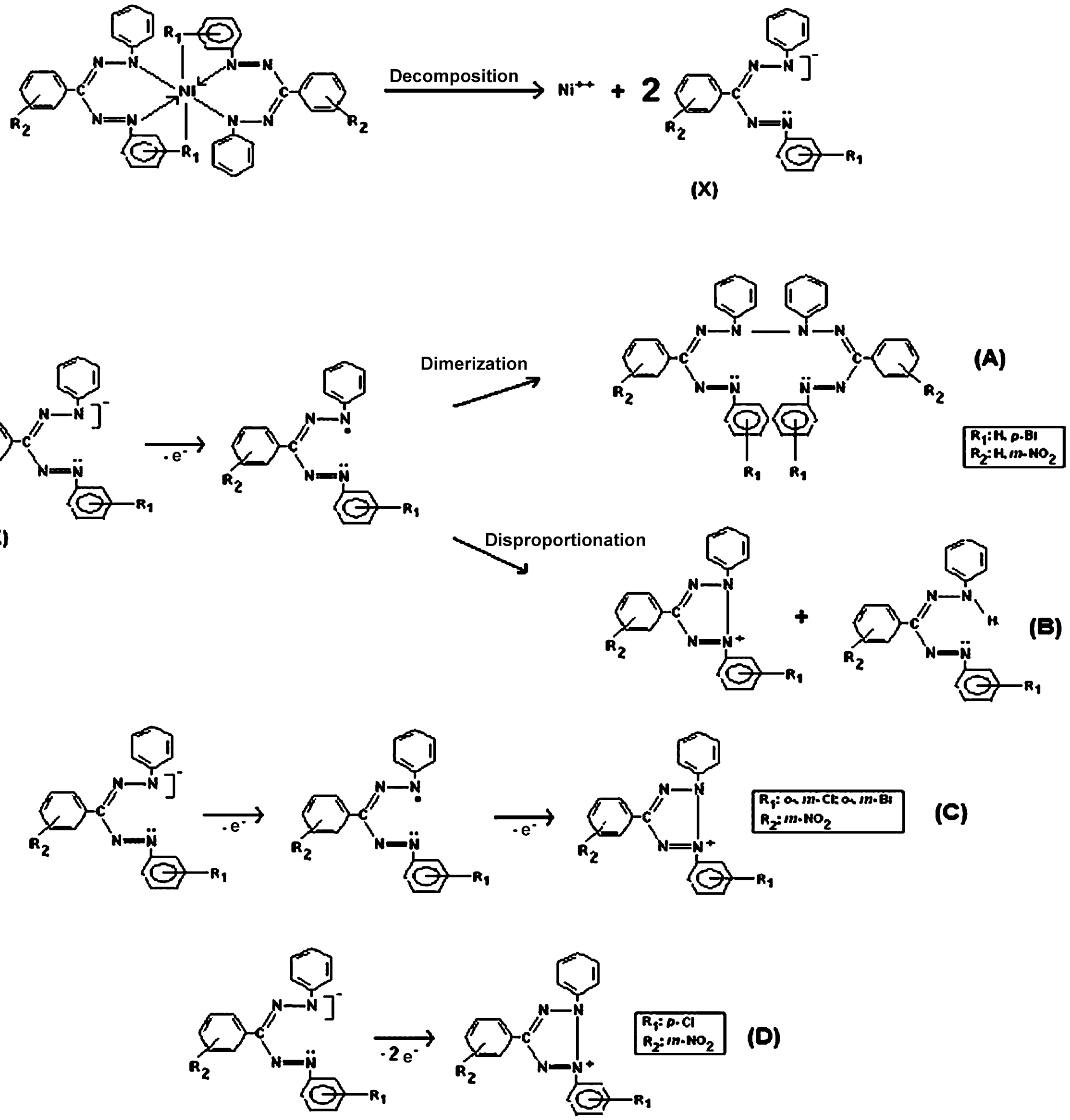

Scheme 3. Possible oxidation mechanisms of Ni(II) complexes formazans.

## 4. Conclusions

Nickel(II) complexes of formazans were prepared and characterized. Their absorption and redox behavior were discussed. Their peak potentials, diffusion coefficients and a number of electrons transferred were determined. Mechanisms of oxidation of compounds showed the effect of changing the type and the position of the substituent on the rings. It was also investigated whether the Hammett substituent coefficients could be used to evaluate the total effect of the two different substituents, upon the $\lambda_{max}$ values and thus the color. Hammett substituent coefficients-$\sigma$ have been related with $\lambda_{max}$ values for only one substituent in the structure up to now. The total $\sigma_T(\sigma_1 + \sigma_2 = \sigma_T)$ and related $\lambda_{max}$ values are in Table 7.

As seen from Fig. 8 there is a linear correlation between Hammet substituent coefficients-$\sigma_T$ and $\lambda_{max}$ values. This shows

Table 7
The total $\sigma_T$ ($\sigma_1 + \sigma_2$) and related $\lambda_{max}$ values

| Substitution position | Compound | Abbreviation | $\sigma'$ values | $\sigma_T$ (total effect) | $\lambda_{max1}$ (nm) |
|---|---|---|---|---|---|
| *m*- | **1b** | H | H: 0 | 0 | 611.0 |
| | **3b** | *m*-Cl, *m*-$NO_2$ | *m*-Cl: 0.37; *m*-$NO_2$: 0.71 | 1.08 | 619.0 |
| | **6b** | *m*-Br, *m*-$NO_2$ | *m*-Br: 0.37; *m*-$NO_2$: 0.71 | 1.08 | 618.0 |
| *p*- | **4b** | *p*-Cl, *m*-$NO_2$ | *p*-Cl: 0.24; *p*-$NO_2$: 0.71 | 0.95 | 624.0 |
| | **7b** | *p*-Br, *m*-$NO_2$ | *p*-Br: 0.26; *p*-$NO_2$: 0.71 | 0.97 | 625.1 |

that it is possible to use the summation of Hammet substituent coefficients-$\sigma_T$ ($\sigma_1 + \sigma_2 = \sigma_T$) to evaluate the absorptional features of the compounds.

## Acknowledgement

We are very grateful to the Gazi University Research Fund for providing financial support for this project (no. 04/2004-13).

## References

[1] J.W. Lewis, C. Sandorfy, Can. J. Chem. 61 (1983) 809–816.

[2] A.R. Katritzky, S.A. Belyakov, D. Cheng, H.D. Durst, Synthesis 5 (1995) 577–581.

[3] H. Tezcan, N. Ozkan, Dyes and Pigments 56 (2003) 159–166.

[4] H. Tezcan, T. Uyar, R. Tezcan, Turk. J. Spect. Aegean Univ. 10 (1989) 82–90.

[5] A.M. Mattson, C.O. Jensen, R.A. Dutcher, Science 5 (1947) 294–295.

[6] V.C. Schiele, Ber. 30 (1964) 308–318.

[7] H. Wan, R. Williams, P. Doherty, D.F. Williams, J. Mater. Sci.: Mater. Med. 5 (1994) 154–159.

[8] K. Umemoto, Bull. Chem. Soc. Jpn. 62 (1989) 3783–3789.

[9] M.I. Viseu, M.L.S. Simoes Goncalves, S.M.B. Costa, M.I.C. Ferreira, J. Electroanal. Chem. 282 (1990) 201–214.

[10] G.M. Abou Elenien, J. Electroanal. Chem. 375 (1994) 301–305.

[11] T. Oritani, N. Fukuhara, T. Okajima, F. Kitamura, T. Ohsaka, Inorg. Chim. Acta 357 (2004) 436–442.

[12] G. Gökce, Z. Durmus, H. Tezcan, H. Yılmaz, E. Kılıc, Anal. Sci. 21 (2005) 1–4.

[13] M. Szymczyk, W. Czajkowski, R. Stolarski, Dyes and Pigments 42 (1999) 227–235.

[14] Y. Gok, M. Tufekci, E. Ozcan, Synth. React. Inorg. Met. -Org. Chem. 23 (1993) 861–873.

[15] D.A. Brown, H. Bögge, G.N. Lipunova, A. Müller, W. Plass, K.G. Walsh, Inorg. Chim. Acta 280 (1998) 30–38.

[16] Y.M. Issa, M.S. Rizk, W.S. Tayor, M.H. Soliman, J. Indian Chem. Soc. 70 (1993) 5–7.

[17] A. Uchiumi, A. Takatsu, H. Tanaka, Anal. Sci. 7 (1991) 459–462.

[18] Y. Kawamura, J. Yamauchi, H. Ohya-Nishiguchi, Bull. Chem. Soc. Jpn. 66 (1993) 3593–3599.

[19] M. Szymczyk, A. El-Shafei, H.S. Freeman, Dyes and Pigments 71 (2006) 206–213.

[20] A.S. Baranski, W.R. Fawcett, C.M. Gilbert, J. Am. Chem. Soc. 57 (1) (1985) 166–170.

[21] R.J. Klingler, J.K. Kochi, J. Phys. Chem. 85 (1981) 1731.

[22] D.H. Williams, I. Fleming, Spectroscopic Methods in Organic Chemistry, McGraw-Hill Publishing Company Limited, London, 1966.

[23] F. Schiman, Nuclear Magnetic Resonance of Complex Molecules, vol. 1, Vieweg and Sohn GmbH, Braunschweig, 1970.

[24] L.J. Bellamy, The Infrared Spectra of Complex Molecules, Methuen, London, 1962.